Symposium on Macroscopic Features of Heavy-Ion Collisions, Argonne, Illinois, April 1-3, 1976)

CONF-760424--2

POTENTIAL MODEL DESCRIPTION OF HEAVY ION ELASTIC AND INELASTIC SCATTERING

G. R. Satchler
Oak Ridge National Laboratory*
Oak Ridge, Tennessee 37830

NOTICE
This report was prepared as an account of work sponsored by the United States Government. Neither the United States nor the United States Energy Research and Development Administration, nor any of their employees, nor any of their contractors, subcontractors, or their employees, makes any warranty, express or implied, or assumes any legal liability or responsibility for the accuracy, completeness or usefulness of any information, apparatus, product or process disclosed, or represents that its use would not infringe privately owned rights.

1. INTRODUCTION

Let us start by asking what we mean by the potential between two nuclei or heavy ions. It is not uniquely defined and failure to remember this has sometimes led to confusion. The conventional optical model potential U(r) for two nuclei a+A is one which appears in a one-body Schrödinger equation,

$$\left[-\frac{\hbar^2}{2\mu}\nabla^2 + U(r)\right]\chi(r) = E\,\chi(r), \tag{1}$$

and whose solution $\chi(r)$, with the appropriate boundary conditions, describes the elastic scattering of a+A. One standard way of justifying Eq. (1) is to expand the total wavefunction Ψ_α of the a+A system in terms of the internal eigenstates of the separate a and A systems,

$$\Psi_\alpha = \sum_{ij} \psi_{ai}\,\psi_{Aj}\,\chi_{ij}(r), \tag{2}$$

where the coefficient $\chi_{ij}(r)$ describe their relative motion. For elastic scattering we are interested in χ_{oo} and by projecting out this term (e.g., Ref. 1) from the total Schrödinger equation $(H-E_\alpha)\Psi_\alpha = 0$ we obtain an equation for χ_{oo} which is of the form (1) with an effective potential $\mathcal{V}$,

$$\mathcal{V} = V_{oo} + \sum_{\alpha\alpha'} V_{o\alpha}\left(\frac{1}{E-H+i\epsilon}\right)_{\alpha\alpha'} V_{\alpha' o}, \tag{3}$$

where V is the true interaction between a and A, and the sum over α is over the excited states of these two nuclei. (Antisymmetrisation makes the equation a little more complicated.) The first term is real and is simply the so-called folded potential. The remainder arises from coupling to all the other states and is complex, non-local, energy- and angular momentum-deperdent. In practice we approximate this $\mathcal{V}$ by a local, complex model potential, U(r), for example

DISTRIBUTION OF THIS DOCUMENT IS UNLIMITED

*Research sponsored by the U.S. Energy Research & Development Administration under contract with Union Carbide Corporation.

By acceptance of this article, the publisher or recipient acknowledges the U.S. Government's right to retain a nonexclusive, royalty-free license in and to any copyright

of Woods-Saxon form.

The point is that, defined in this way, this potential $\mathcal{V}$ (and by implication the equivalent model U) describes the relative motion in that component of the total wave function Ψ in which the two nuclei remain in their ground states (χ_{oo} in Eq. (2)). Strong absorption into other channels manifests itself through χ_{oo} becoming very small when the nuclei overlap and $\mathcal{V}$ being strongly absorbent there.

This is quite different from most of the potentials calculated for heavy-ion collisions. These calculations attempt to follow, to a greater or lesser degree, the readjustments that the two ions must make as they begin to interact. These readjustments include an increase in internal kinetic energy[2] due to the Pauli principle as the two Fermi fluids overlap, a reduction in the internal potential energies as the densities overlap[3] (saturating property of nuclear forces), both of which lead to a repulsion at small distances, and changes in shape.[4] In other words, these calculations are not just concerned with the χ_{oo} component of Eq. (2) but include a wide range of excited states (of the separated systems) also. The (real) potential obtained is not simply related to $\mathcal{V}$ or the U that appears in Eq. (1). In particular, although some aspects of the coupling to other channels (other terms in the sum (2)) are taken into account explicitly in these calculations, it is not clear, to me at least, how the loss of flux to these channels (the absorptive potential) is to be handled. Consequently one must be careful in relating these calculated potentials to optical potentials empirically determined from elastic scattering.

In addition, these calculations imply modifications of the kinetic energy of relative motion as well as the potential energy. This was stressed by Mosel (in a paper[5] unfortunately published in a rather short-lived journal). Using as an example a collective model Hamiltonian, he pointed out that the inertial parameters are not independent of the coordinates; i.e. the kinetic energy term differs from that in Eq. (1). He showed that in this case the Schrodinger equation could be rearranged into the form (1), but at the expense of modifying the calculated potential and adding an L-dependent term. The modifications vanish when the two nuclei are separated, but can be important in the overlap region.

We may expect that most of the non-locality of the potential operator can be converted to an equivalent local but energy-dependent potential. We can also anticipate angular-momentum (and parity) dependence in the local

potential. The shape of the equivalent potential U(r) need not be Woods-Saxon in form. Heavy ions with their shorter wavelength will explore more localised regions of the potential than do light ions (but see Ref. 6 however) and may be sensitive to these shape differences. (Indeed, there are some indications[7] that the square of a Woods-Saxon form factor gives a better account of $^{12}C + ^{12}C$ scattering than the Woods-Saxon itself.)

If the coupling between the entrance channel and one or a few exit channels is strong, it may be that the non-locality and angular momentum structure of the corresponding contributions to $\mathcal{V}$ of Eq. (3) cannot easily be represented by a simple local potential U(r). In that case it may be necessary to take these channels into account explicitly (take two or more terms in the expansion (2) if the strong reactions are inelastic scattering) by solving the corresponding set of coupled equations instead of the single Eq. (1). Two words of caution. Having the total non-elastic cross section comparable to or larger than the elastic does not in itself invalidate the use of the optical model; the non-elastic cross section may be composed of many contributions whose overall effect can be represented by a simple local potential. Only if some feature of each contribution is correlated in some way (such as may occur if they are all peripheral, direct reactions) is there likely to be trouble. Further, although having the non-elastic cross section for one particular channel comparable to the elastic cross section often means trouble, even here there is no á priori guarantee that a simple one-channel potential will not suffice. Usually the best arguments for solving coupled equations are that (i) the parameters can be more easily given a physical interpretation and (ii) one wants a simultaneous, consistent fit to elastic and non-elastic data.

2. PHENOMENOLOGY AND THE DATA

I wish I could give you a coherent picture of the optical model analysis of heavy-ion scattering, for example by quoting a global set of parameters, but we just are not there yet. As is well known, there are tremendous ambiguities associated with the potentials for the scattering of strongly absorbed systems which, except for the lightest nuclei and the highest energies, are only sensitive to the extreme tail of the potential. There is perhaps some hope that the folding model for the real potential, discussed below, will help here. I have not, as yet, seen any systematic behaviour of the preferred

parameters for the imaginary potential, except as a function of energy.

What do the data determine? Typically they tell us[8-10] the strength of the real and imaginary potentials at the strong absorption radius, $r = D_{1/2}$, (= distance of closest approach for the Rutherford orbit which has the same L as the partial wave for which $T_L = 1/2$). ReU is usually around 1 MeV at this point. The data also place some constraints on the slope of the potential in this region; typically $a \sim 0.6$ fm if we represent ReU here by $\exp(-r/a)$. Usually this information can be embodied adequately in a 4-parameter Woods-Saxon (WS) potential and even this has one redundant parameter which needs to be fixed somewhat arbitrarily.

When the scattering angular distribution has the characteristic form of Rutherford, followed by Coulomb-nuclear interference oscillations about Rutherford, followed by an exponential fall below Rutherford, it is very important to have complete and accurate data in the region of oscillation about Rutherford. For example, this region is critical in determining the strength of the imaginary potential near $r = D_{1/2}$; the larger the amplitude of oscillation, the smaller the ImU needed.[9,11] Figure 1 shows this in the context of using a 4-parameter WS potential with V fixed at 40 MeV and r_o, a adjusted for optimum fit. (It is easy to miss this kind of information unless the data are well defined in this region and unless they and the optical model analysis are subjected to close scrutiny. In particular, the practice of plotting the cross sections semi-logarithmically obscures the quite small differences in this region; for this purpose, a linear plot is to be preferred.) The result of this kind of analysis for a variety of systems is that ReU and ImU have comparable magnitudes at the strong absorption radius (see Fig. 2), for bombarding energies around 10 MeV/nucleon. There are also indications[12] that the ImU/ReU ratio is strongly energy dependent for lower energies. Figure 3 shows results for ^{16}O + Ni, data for which are available over a wide range of energies. Although the decrease in ImU as the energy falls appears to be very dramatic, the variation in the mean free path Λ near $r = D_{1/2}$ is not so great because the local kinetic energy T (all rotational at this point) is also decreasing;

$$\Lambda(r) \approx 1.3\ T(r)^{1/2}/\mathrm{ImU}(r)$$

in fm if T and U are in MeV. Even at the highest energy, $\Lambda \sim 10$ fm at $r = D_{1/2}$.

Figure 3 also shows that $D_{1/2}$ does not vary much with energy, about

0 6 fm over this range, so that the elastic scattering only probes a limited region in the surface. If we assume there is an underlying energy-independent real potential, then the fits at different energies allow us to map out ReU as a function of distance; this is shown in Fig. 4. The points scatter too much to determine the slope precisely, but they are consistent with $\exp(-r/\alpha)$, $\alpha \sim 0.65$ fm. (The lines in Fig. 4 are folded potentials to be discussed below.)

3. DEEP OR SHALLOW POTENTIALS?

A popular question about optical potentials for heavy-ion scattering is: "Are they deep or shallow?". Of course, the question is meaningless when the data are only sensitive to the extreme tail of the potential. For example, Fig. 5 shows that the data[9] for $^{16}O + {}^{208}Pb$ at 192 MeV cannot distinguish between a potential which is 10 MeV deep and one which is 600 MeV deep provided the extreme tails are similar. The potentials are shown in Fig. 6; in this case the available data do not probe the potential closer than about 11 fm. It was suggested[13] that, by analogy with analyses of alpha particle scattering, data taken at sufficiently high energy and/or on lighter systems (and out to sufficiently large scattering angles -- beyond the nuclear rainbow angle) would probe more deeply and distinguish between deep and shallow potentials.

$^{16}O + {}^{28}Si$ seemed a good system to try out these ideas and there are now data available from 33 to 215 MeV. Cramer, et al.[14] searched for an energy-independent WS potential to fit all these data simultaneously. Their results showed that to do this required a shallow potential, called E18, with a real depth of about 10 MeV. The fits are shown in Fig. 7. In this case, the strong absorption radius at 215 MeV is about 8.2 fm, but they were able to show that the scattering at that energy was sensitive to variations in the potential into about $5.5 \approx 1.0\ (A_1^{1/2} + A_2^{1/2})$ fm where the real potential is about -9.6 MeV.

I found this result challenging so I looked for an equally good fit using a folded real potential (see below) which is about 530 MeV deep, plus a WS imaginary potential. This could be done if the diffuseness of the imaginary potential was allowed to increase linearly with energy (but still with one less parameter than used by Cramer, et al.). Figure 7 shows that the data are

equally well fitted. However, the two potentials are not identical in the surface region; by 5.5 fm, the folded potential is 51 MeV deep. Neither are the predicted cross sections identical; in particular, the WS potential E.18 predicts slightly larger oscillations about the Rutherford value at small angles and concomitantly it predicts smaller absorption cross sections (10% less at 38 MeV, 20% less at 215 MeV). Unfortunately, the data at the two highest energies do not extend into these small angles.

What we conclude from this is that this particular set of data, extensive though it may be, cannot distinguish between a shallow WS potential and a very deep potential with a different shape in the surface.

Another system for which there is much data is $^{12}C + ^{12}C$, detailed angular distributions being available for various energies up to 127 MeV. Analyses[15] showed that while the shallow potentials introduced by the Yale group gave adequate fits to new 70-127 MeV data[16] for angles less than about 45°, no good fit to the larger angles was found with WS potentials. However, the use of deep folded potentials resulted in a marked improvement (Fig. 8). In this case the scattering is sensitive to the potential as close in as $3 = 0.66\ (A_1^{1/3} + A_2^{1/3})$ fm where ReU is well over 100 MeV deep, although the strong absorption radius is about 7 fm. Again the folded potential has a shape which cannot be closely matched by a WS form in this 3-7 fm region. On the other hand, the folded potential is closer in shape to the square of the WS form; this form can also be used to fit the data and such fits also result in a deep potential.[7] Consequently we must conclude that, within the context of these simple potential wells, the $^{12}C + ^{12}C$ data require a deeper potential than had been thought previously.

4. FOLDED POTENTIAL MODELS

The first term V_{oo} of the formal expression (3) for the optical potential consists simply of the basic nucleon-nucleon interactions between the two nuclei folded into the density distribution $\rho(r)$ of each nucleus. (Antisymmetrisation introduces exchange terms also which we shall ignore for the present.) We may hope that this term V_{oo} by itself is a reasonable approximation for the extreme tail of the real potential because the other terms tend to have shorter ranges. (A possible exception to this argument is that the long-ranged Coulomb forces may distort the nuclear density distributions as

the ions approach one another.) This is the basis of the folding models[8] for the real potential. The imaginary potential is usually treated phenomenologically (but see Ref. 18). The folding models appear in two guises:

4.1 Single-folding

This form has been used by many people; it takes an optical potential $U_N(r)$ for the scattering of a nucleon from one nucleus and folds this into the density distribution of the other nucleus. This I call the single folding model.[8] One may then choose the parameters of $U_N(r)$ empirically from fits to nucleon-nucleus scattering. This procedure overestimates the heavy ion real potential near the strong absorption radius by a factor of two or more;[8,17] i.e. it will not fit observed elastic scattering. A potential of this form was used by Brink and Rowley[19] and their results, when examined closely, support my conclusion.[8,17] It will be interesting to learn the reason for this failure of the single-folding model, since the first term V_{oo} of Eq. (3) is not a bad approximation to the nucleon-nucleus potential itself. It is possible that the Woods-Saxon shape taken for the nucleon-nucleus potential, while quite adequate for nucleon scattering which is not sensitive to the tail of the potential, is inadequate for use in the folding procedure for heavy ions where the tail becomes more important. It might be interesting to repeat some single folding calculations using a form like the $(\text{Woods-Saxon})^2$ with the same surface thickness but a shorter tail.

4.2 Double-folding

This involves folding an effective nucleon-nucleon interaction v into the density distribution of both target and projectile,

$$U(r) = \int d^3r_1 \int d^3r_2 \; \rho_1(r_1)\rho_2(r_2)v(r_{12}), \tag{4}$$

where $\vec{r}_{12} = \vec{r} + \vec{r}_2 - \vec{r}_1$. We now need v. The bare nucleon-nucleon interaction is too strong to be used itself; we must use Brueckner or multiple-scattering theory to replace it by a G-matrix or effective interaction. In principle v is then complex, non-local, energy- and density-dependent, but in practice it is simplified considerably. There are two main approaches to this which for convenience I call the high-energy and low-energy approaches.

The high-energy approach has been used by Dover and Vary;[18,20] in the high-energy limit (impulse approximation) v would become the (complex)

t-matrix for free space nucleon-nucleon scattering. Then (large) corrections are made approximately for the effects of the nuclear medium in which the two interacting nucleons are embedded, namely Pauli principle, off-shell propagation and the Fermi motion of the nucleons. In practice a simple ansatz is adopted; v is assumed to be local and of Gaussian form and the strength estimated in the way just indicated. The range of the Gaussian is not well determined but has been chosen on "reasonable" grounds to be 1 fm[21] or 1.4 fm.[18] (The choice of range will have important effects on the strength required to fit the data. The volume integral of v is not a good criterion; it does not stay constant with changes in range as it does for nucleon scattering. The elastic data may also impose an upper limit on the range which is acceptable.[9] In addition, the relative strengths of different multipoles in inelastic scattering depends upon this range.[22])

The low-energy approach notes that most heavy-ion scattering data currently available are for quite low energies (~5 to 10 MeV/nucleon) and assumes that the effective interaction is similar to the G-matrix for two nucleons bound near the Fermi surface. This approach has been used with some success for nucleon elastic and inelastic scattering. The two most recent attempts to follow this program obtain a local v. One[23] consists of finding a sum of three Yukawa terms which will reproduce the G-matrix elements in an oscillator basis of either the Reid potential or those deduced from nucleon-nucleon scattering by Elliott, et al. One Yukawa was chosen to be the OPEP, another to have a range of 0.4 fm based upon recent OBEP's which simulate multiple-pion exchange. The shortest range of 0.25 fm was chosen somewhat arbitrarily. The OPEP is fixed but the strengths of the other two components were varied. This procedure leads to odd-state interactions whose low momentum (Fourier) components (aside from the OPEP contribution) are like those of a zero-range force. A true zero-range odd-state force would not contribute because the exchange terms (due to antisymmetrisation) would cancel the direct terms; on this basis we include only the OPEP part of the odd-state interaction. However, the OPEP does not contribute because of spin, isospin averaging if both N and Z are even for either ion. This means the OPEP contribution from the odd-state force is cancelled by the OPEP part of the even-state force. We are left with the remainder of the even-state interaction which, for the fit to the Reid G-matrix, is just

$$v = \left[6315 \frac{e^{-4r}}{4r} - 1961 \frac{e^{-2.5r}}{2.5r}\right] \text{MeV}. \tag{5}$$

The other recent work[24] was done for an application of the folding model to alpha particle scattering. Now $G\phi = V\psi$, where ϕ and ψ are the uncorrelated and correlated two-nucleon wavefunctions, respectively. Then a local potential equivalent to G is simply

$$v(r) = V(r)\psi(r)/\phi(r). \tag{6}$$

This was evaluated numerically for the Reid soft core potential and various densities of nuclear matter. I have only made a few tentative calculations with the v appropriate for 5% of normal nuclear density, treating it in the same way as above, i.e. only including the non-OPEP part of the even-state interaction. It gives folded potentials near the strong absorption radii very close to (roughly 10% deeper than) those obtained from the interaction (5). Adding the non-OPEP odd-state interaction from (6) only adds another 10% to the depth in this tail region so that our cavalier treatment of this contribution in deriving (5) does not seem likely to be the source of severe error.

In addition to uncertainties in the interaction, there are also uncertainties in our knowledge of the density distributions $\rho(r)$ to be used in the convolution (4). Electron scattering tells us, in some cases, about the <u>charge</u> distribution; the finite size of the proton has to be unfolded from this in order to yield the distribution of proton centers. (The major effect of the finite size is to make the charge distribution more diffuse than the center distribution. The proton MSR is between 0.64 and 0.85 fm^2. In addition, there should be corrections for the neutron charge and for exchange currents.[25])

Further, electron scattering does not give accurate information on the extreme tail of the density distribution (typically we need to know ρ out to where it is less than 10^{-4} of the central density in order to evaluate (4) accurately at the strong absorption radius. This means going at least 10 times the surface diffuseness beyond the half-density radius if the WS form is used). In addition, we have <u>no</u> accurate information about neutron distributions; the current consensus seems to be that the neutron and proton distributions are similar for N=Z nuclei but that the neutrons in heavier nuclei probably have RMS radii about 1/10 fm greater than do the protons. The best

approach perhaps is to use the independent particle model with parameters adjusted to give the best agreement with electron scattering (or Hartree-Fock calculations if they give agreement). If, in addition, information from neutron and proton pick-up experiments is used, at least the contribution to the density from the last-filled major shell can be estimated quite accurately (this gives about 2/3 of the folded potential at the strong absorption radius in the case of $^{16}O + ^{208}Pb$). Use of the shell model implies one should also apply a center-of-mass correction, but this appears to be small except for the very lightest nuclei. Figure 9 indicates the importance of these matters; the predicted potential at the strong absorption radius is plotted against the sum of the RMS density radii for a variety of density choices. (As the scatter in the points indicates, there is not an exact correlation with the RMS radius, but it is a convenient indicator of the nuclear sizes.) Here, except in one case, we assumed equal neutron and proton distributions. The uncertainty in the results from electron scattering is indicated; it corresponds to about ± 20% uncertainty in the potential, about half of which arises from uncertainty in the size of the proton itself!

Finally, we should remind ourselves that the expression (4) for the folded potential ignores exchange of nucleons between the two nuclei due to antisymmetrisation. Sinha's calculations[3] indicated a very small exchange effect at the strong absorption radius but recent estimates[24] for alpha scattering give a 30% increase in the potential due to exchange. This needs to be explored further for heavy ions.

4.3 Fits to data

When testing the folded potential models against experiment, one must decide what to do about the imaginary, absorptive potential. The high-energy approach automatically generates a complex interaction. The applications which have been made[18,20,21] have assumed for simplicity that the ranges of the real and imaginary parts were the same. This seems to have worked satisfactorily, although in general one would expect different ranges. The low-energy approach, being based upon bound state properties, does not immediately give an imaginary part. So far it has been added phenomenologically, either by multiplying the folded potential by a complex number or by adding an imaginary WS term. There are cases where it is not sufficient to have the same shape for the real and imaginary parts ($^{16}O + ^{28}Si$ was one of these)

indicating that a different range (or a different dependency on the density) is needed for the imaginary part of v.

Applications of both high- and low-energy approaches have been very successful[7-9,18,20-22] (see also Figs. 5, 7, and 8) in fitting elastic data. This is not too surprising in those cases where the scattering is sensitive only to the value of the potential at the strong absorption radius if the strength of the interaction is treated as a completely free parameter,[8,9,20,21] although the model is still valuable in that there is only one adjustable parameter rather than three, as in the WS potential. Of course, the model may still have predictive power if the interaction strength required is found to be mass- and energy-independent. (This appears to be the case for the Gaussian interaction which fits low-energy nucleon-nucleon scattering.[9,17] Data for systems ranging from $^{12}C + ^{12}C$ to $^{20}Ne + ^{208}Pb$ have been fitted, all needing approximately the same renormalisation factor for the interaction strength of $N \approx 0.6$.)

However, renormalisation does not seem to be required for some interactions. Figure 10 shows some results[18] using what I called the high-energy approach in which, for the elastic scattering, all parameter values were essentially pre-determined and only the deformation parameters of the densities were adjusted for the inelastic (the deformation lengths obtained being in good agreement with electromagnetic values).

The interaction (5) obtained in the low-energy approach also has had many successes. Optimum fits to the data have been obtained with no more than about ± 10% renormalisation of its strength. (The uncertainties discussed above in the density distributions to be used can result in variations of this order.) Figures 7 and 8 are examples. Figure 11 shows another, for $^{40}Ca + ^{40}Ca$, in which the imaginary potential was assumed to be the same (folded) shape as the real and its strength was the only parameter to be adjusted. (Although the fit is impressive for a one-parameter model, the deviation from the data at the forward angles is significant and must be studied further. A four-parameter WS potential is able to fit this region.) As mentioned previously, the interaction (6) of Day, et al.[24] has similar success.

The first signs of possible failure of this model occur when it is applied to heavy systems like $^{40}Ar + ^{238}U$ or $^{84}Kr + ^{209}Bi$. Empirically[26] the data for these systems seem to indicate that the potential at the strong absorption radius remains around 1 MeV independent of the masses. Further this

critical radius continues to occur when the nuclei are separated by a constant distance (about 3 fm between the half-central-density points). The folding model predicts the interaction potential at this radius to increase as the systems get larger (just as the proximity potential[27] increases proportional to the geometric mean of the radii of the two nuclei). Consequently, the interaction (5) for example predicts -ReU to be between 4 and 5 MeV for ^{84}Kr + ^{209}Bi instead of the 1.1 MeV deduced from the data. It may be that the very strong Coulomb forces acting between these systems invalidates the use of a "frozen" or undistorted density in the folding calculation. It is also true that the elastic data for these cases are much more difficult to obtain and consequently they are less certain.

5. INELASTIC SCATTERING

I will not dwell upon the many successful applications of the standard collective model prescription in which the optical potential itself is deformed and the non-spherical parts used to induce inelastic scattering. I only mention one recent application[28] to the scattering of ^{12}C from the Nd isotopes, ranging from "spherical" to strongly deformed. The spherical optical potential could produce fits to the elastic scattering from the most strongly deformed isotope but at the expense of somewhat unphysical parameter values which differed appreciably from those for the spherical isotope. However, the use of coupled-channel calculations which take the deformation into account explicitly removed this difficulty and a single optical potential was found for all the isotopes.

Of particular interest is the extension of the folding models to inelastic events. This may be done within the collective model, but deforming the nuclear density instead of the potential and then folding in the effective interaction. This has been used successfully in the high-energy approach,[18,21] one example being Fig. 10. It has also been used with the interaction (5), as shown for example in Fig. 12. In this case the renormalisation factor N = 1.1 had been determined by analysis of data at 142.5 MeV; Fig. 3 indicates we can expect a smaller absorptive strength at the lower energy of 61.4 MeV and only this one parameter was varied to produce the elastic fit shown. This same complex interaction (i.e. (1.1 + 0.6i) times interaction (5)) was then folded into the deformed density of ^{60}Ni; the deformation

parameter was determined from the known B(E2) value for this transition, and it was assumed that neutrons and protons contributed in the ratio N/Z. The predicted inelastic scattering is seen to be in good agreement with the measurements.

When the appropri. e electron scattering data are available, the charge transition density may be known in more detail (usually in some parameterised form). Unfolding the finite size of the proton gives the proton transition density; if N = Z we may assume that the neutron transition density is similar for the strong isoscalar transitions to low-lying excited states. This was done for the ^{12}C excitation[7] shown in Fig. 8, using the interaction (5). It has also been applied successfully to excitation of the 2^+ state in ^{28}Si by ^{16}O ions.

In some cases there are available microscopic (e.g. 1-particle, 1-hole RPA) calculations of the transition densities. The proton parts of these may be checked against electron scattering and measured B(EL) values. These have been used[22] for inelastic ^{12}C scattering from ^{208}Pb (see Fig. 13), not using the more recent interaction (5) but using Gaussians normalised to fit the elastic scattering. Evidence was found that the inelastic scattering favoured the choice of a range of about 1 fm, partly based upon the relative cross sections for different multipoles and partly upon their angular distributions.

All the cases just discussed were calculated using the DWBA. When the coupling is strong, this may not be adequate (and higher-order feedback may affect the elastic scattering also), and it becomes necessary to solve coupled equations. This has been explored to some extent[7] for $^{12}C + {}^{12}C$ using the folding model.

6. FINAL REMARKS

I have put particular stress upon the folding model approach. This model seems reasonable for the distant collisions which are important for determining the elastic scattering, although even here we must recognise that there is a strong Coulomb field acting. When the nuclei approach more closely, the folded potential loses its simple physical significance; certainly it should not be identified closely with the potentials which determine fusion barriers, etc., although it should agree with them asymptotically. However, it is a nice simple model which has had successes and it seems worth pursuing until we

see where it breaks down and what we can learn from that.

The success of this interaction (5) as compared to the relative failure[17] of previous attempts in this direction appears to be largely due to the shorter range of this interaction, resulting from a proper elimination of the OPEP tail and recognition of the short ranges associated with multiple-pion exchange.

The failure of the single-folding model is still not understood but may be connected with deficiencies in the WS shape for nucleon-nucleus optical potentials.

There are many aspects of elastic and inelastic scattering that I have not touched upon but -- another place, another time!

ACKNOWLEDGMENTS AND APOLOGIES

I am indebted to numerous experimentalists who have sent me tables of elastic cross sections; they have been very helpful.

Some of the figures reproduced here were, for lack of time, drawn by myself; my apologies to the ORNL Graphic Arts Department. Lack of time also led to most of the figures chosen being from readily available ORNL work.

REFERENCES

1. See, for example, H. Feshbach, Ann. of Phys. (N.Y.) 19, 287 (1967).
2. See, for example, P. G. Zint and U. Mosel, Phys. Lett. 56B, 424 (1975).
3. See, for example, C. Ngô, et al., Nucl. Phys. A240, 353 (1975); B. Sinha, Phys. Rev. C11, 1546 (1973).
4. See, for example, A. S. Jensen and C. Y. Wong, Nucl. Phys. A171, 1 (1971).
5. U. Mosel, Particles & Nuclei 3, 297 (1972).
6. D. A. Goldberg, Phys. Lett. 53B, 59 (1975).
7. L. D. Rickertsen, et al., contribution to this meeting.
8. G. R. Satchler, p. 171 in Procs. Conf. on Reactions Between Complex Nuclei, Nashville, 1974 (North-Holland Publishing Co., 1974) Vol. 2.
9. J. B. Ball, et al., Nucl. Phys. A252, 208 (1975).
10. P. J. Moffa, C. B. Dover, and J. P. Vary, Phys. Rev. C13, 147 (1976).
11. G. R. Satchler, Phys. Lett. 55B, 167 (1975).
12. G. R. Satchler, Phys. Lett. 58B, 408 (1975).
13. D. A. Goldberg and S. M. Smith, Phys. Rev. Lett. 33, 715 (1974).
14. J. G. Cramer, et al., to be published.
15. R. M. Wieland and R. G. Stokstad, private communication.
16. R. M. Wieland, et al., ORNL Annual Report (1975).
17. G. R. Satchler, Phys. Lett. 59B, 121 (1975).
18. P. J. Moffa, et al., Phys. Rev. Lett. 35, 992 (1975).
19. D. M. Brink and N. Rowley, Nucl. Phys. A219, 79 (1974).
20. J. P. Vary and C. B. Dover, Phys. Rev. Lett. 31, 1510 (1973).
21. C. B. Dover, P. J. Moffa, and J. P. Vary, Phys. Lett. 56B, 4 (1975).
22. G. R. Satchler, et al., Phys. Lett. 60B, 43 (1975).
23. G. Bertsch, et al., to be published; W. G. Love, private communication.
24. Y. Eisen, B. Day, and E. Friedman, Phys. Lett. 56B, 313 (1975); Y. Eisen and B. Day, to be published.

25. Il-Tong Cheon, Phys. Lett. 60B, 409 (1976).

26. See, for example, J. R. Huizenga, previous talk.

27. See, for example, W. D. Myers, p. 1 in Procs. Conf. on Reactions Between Complex Nuclei, Nashville, 1974 (North-Holland Publishing Co., 1974) Vol. 2.

28. D. L. Hillis, et al., Bull. Am. Phys. Soc. 20, 1192 (1975) and to be published.

29. H. Doubre, et al., Phys. Rev. Lett. 35, 508 (1975).

30. K. E. Rehm, et al., Phys. Rev. C12, 1945 (1975).

31. P. Ring and J. Speth, Nucl. Phys. A235, 315 (1974).

FIGURE CAPTIONS

Fig. 1. Illustrating the importance of the forward angles for determining the strength of the imaginary potential.[11]

Fig. 2. Variation of χ^2 for fit to data as the imaginary strength W is varied.[11]

Fig. 3. Energy variation of imaginary strength from fitting data with a 4-parameter WS potential.[12]

Fig. 4. Values of the real potential at the strong absorption radius, $r = D_{1/2}$. (The lines correspond to folded potentials with various interactions.[12])

Fig. 5. Effect on the scattering of leveling off (or putting to zero) the real potential[9] at 10 and 11 fm.

Fig. 6. The potential[9] used for the curves shown in Fig. 5. The strong absorption radius here is $D_{1/2} = 12.5$ fm.

Fig. 7. Folded potential fit to $^{16}O + ^{28}Si$, using the interaction (5) renormalised by N = 0.9. The WS potential E18 is due to Cramer, et al.[14]

Fig. 8. Preliminary fit to $^{12}C + ^{12}C$ using the interaction (5) renormalised by N = 1.1. The data[16] normalisation is also preliminary and may later change by a few per cent.

Fig. 9. Variation of the folded potential at the strong absorption radius ($D_{1/2} = 10.4$ fm) for $^{40}Ca + ^{32}S$ with the sum of the RMS radii for the two density distributions. (The dashed line is drawn to guide the eye.)

Fig. 10. Folded potential fit[18] to ^{14}N elastic and inelastic scattering from light nuclei.

Fig. 11. A one-parameter folded potential fit to $^{40}Ca + ^{40}Ca$ data[29] (solid curve), using the interaction (5) times (1.0 + 0.7i). The dashed curve represents a 4-parameter WS potential fit.

Fig. 12. Fit to $^{16}O + ^{60}Ni$ elastic and inelastic scattering[30] using the interaction (5) times (1.1 + 0.6i).

Fig. 13. Comparison with data[22] for inelastic ^{12}C scattering from ^{208}Pb. The transition densities were obtained from RPA calculations;[31] the interaction was a Gaussian with range 1 fm normalised to the elastic scattering. Either WS or folded imaginary potentials were used.

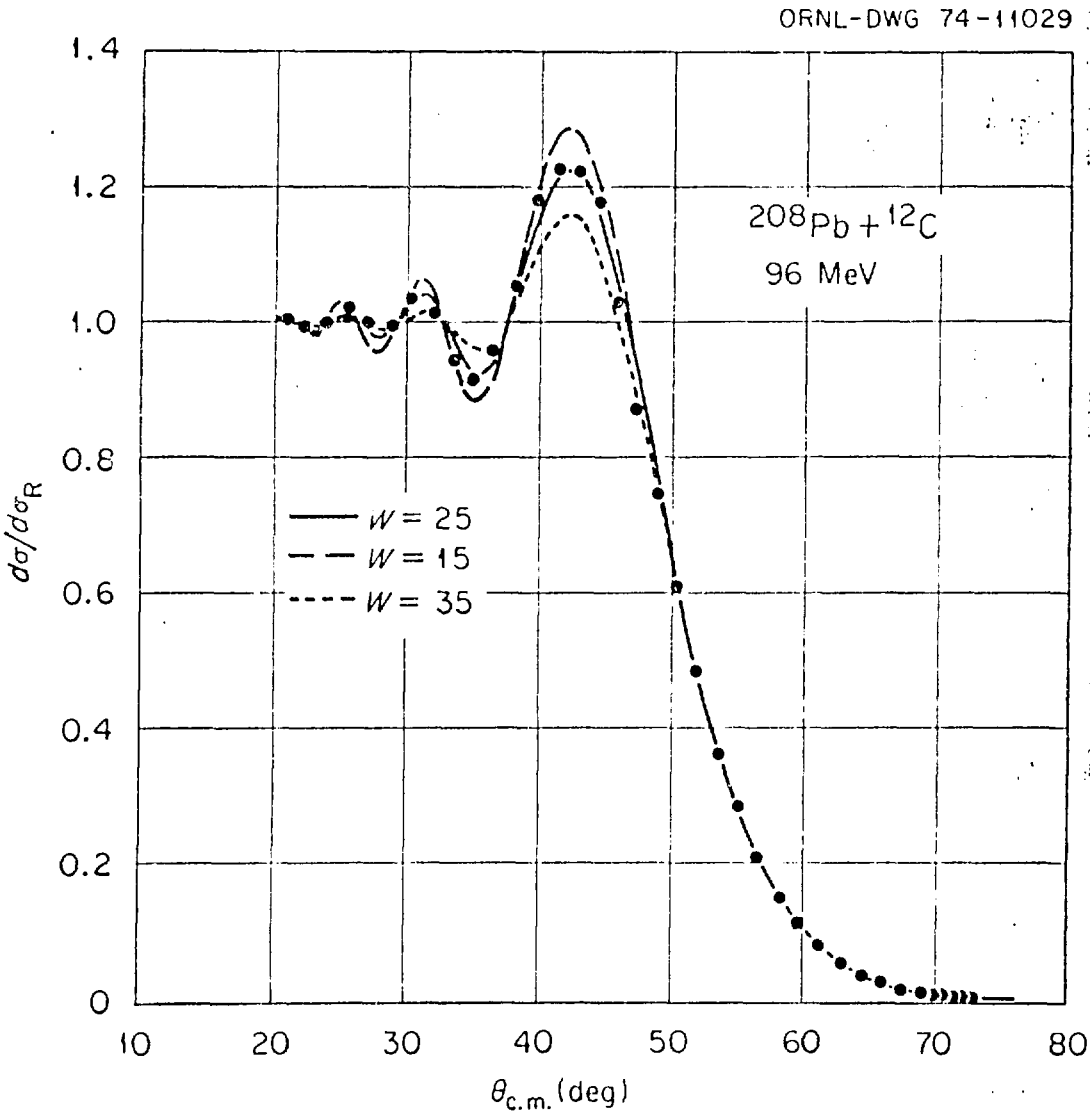
ORNL-DWG 74-11029
$^{208}Pb + ^{12}C$
96 MeV
W = 25
W = 15
W = 35
$d\sigma/d\sigma_R$
$\theta_{c.m.}$ (deg)
1.4
1.2
1.0
0.8
0.6
0.4
0.2
0
10
20
30
40
50
60
70
80

ORNL-DWG 74-11030

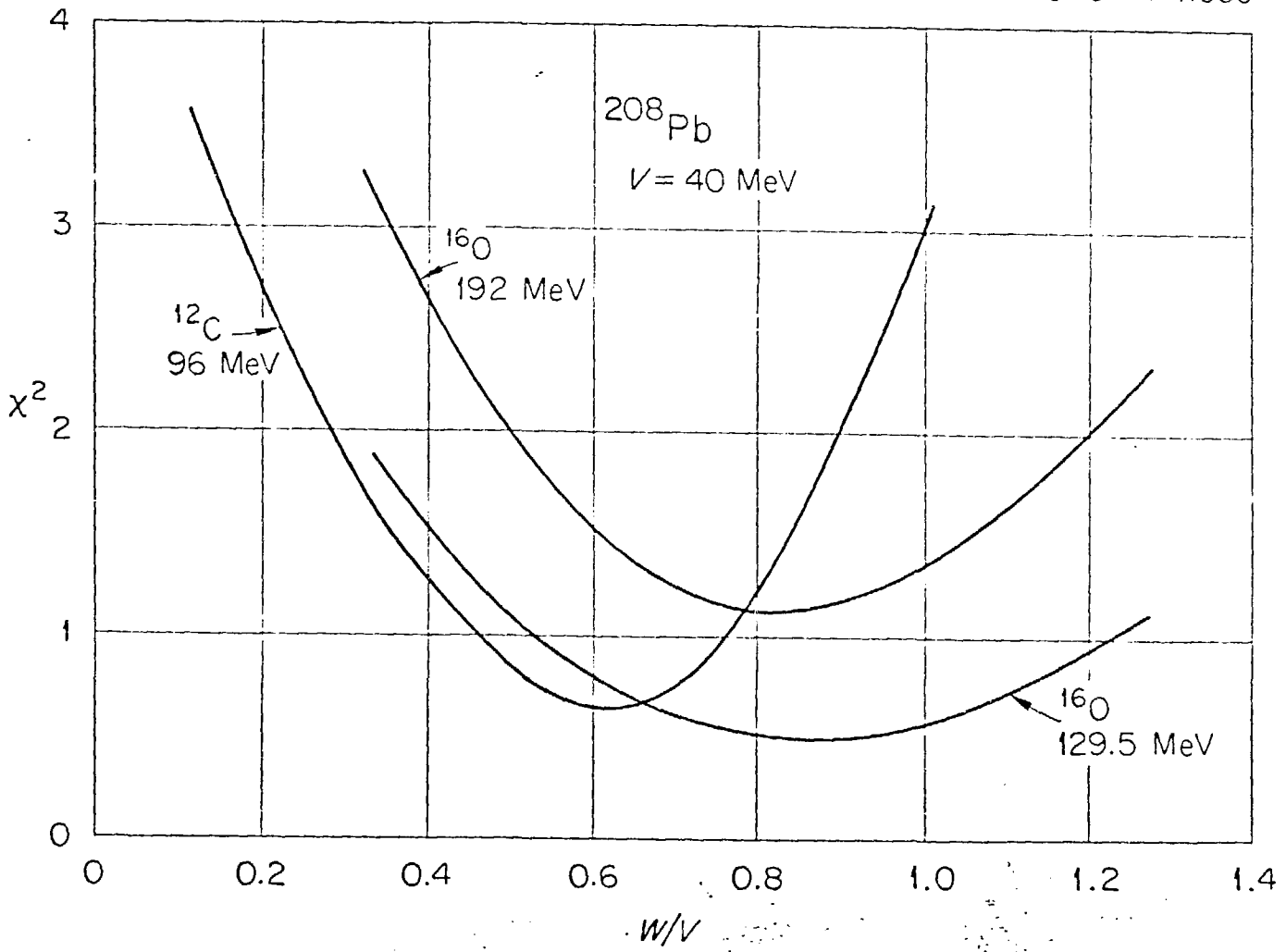

2

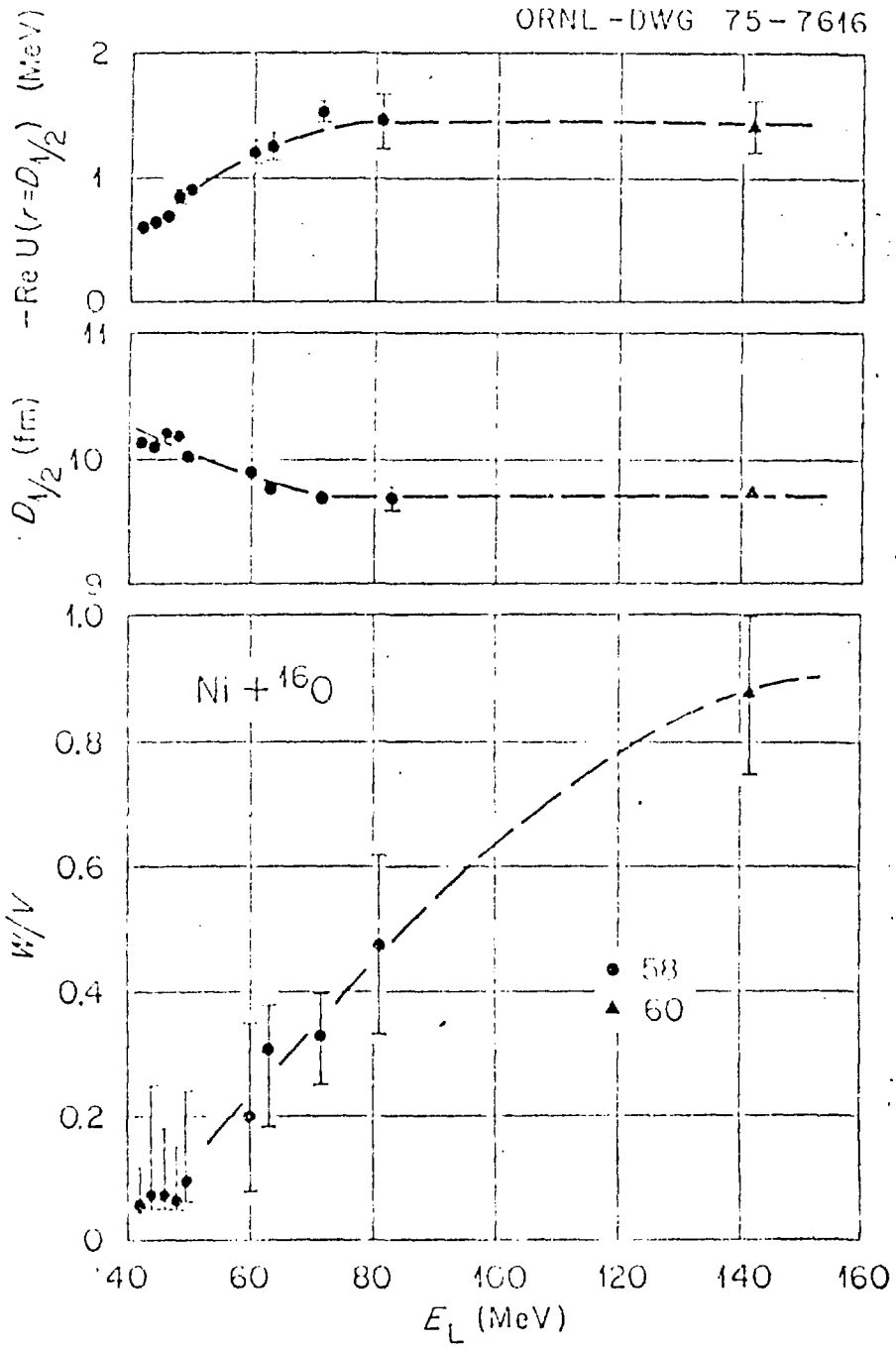
ORNL-DWG 75-7616
$-\mathrm{Re}\,U(r=D_{1/2})$ (MeV)
$D_{1/2}$ (fm)
W/V
$\mathrm{Ni} + {}^{16}\mathrm{O}$
58
60
E_L (MeV)

3

ORNL-DWG 75-7617

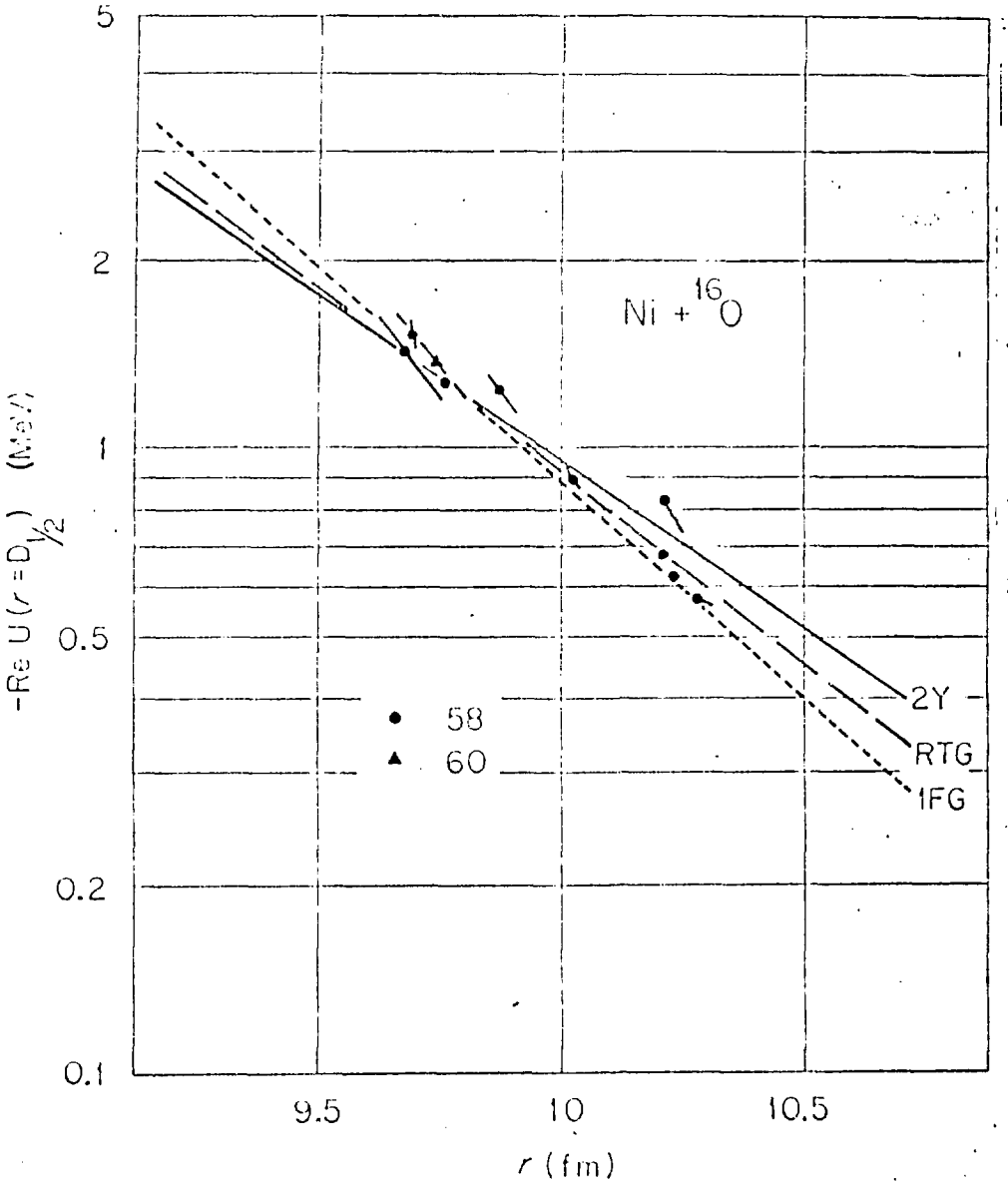

4

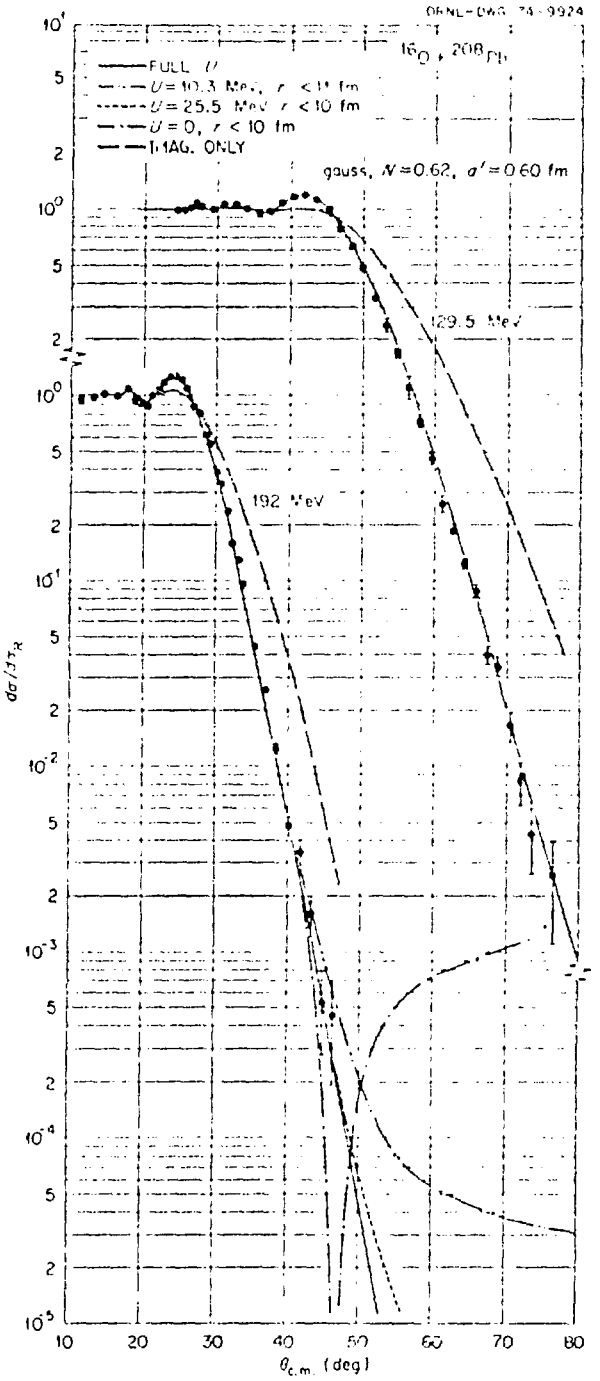
ORNL-DWG 74-9924
$^{16}O + ^{208}Pb$
FULL U
U = 10.3 MeV, r < 11 fm
U = 25.5 MeV r < 10 fm
U = 0, r < 10 fm
IMAG. ONLY
gauss, N = 0.62, a' = 0.60 fm
129.5 MeV
192 MeV
$d\sigma/d\sigma_R$
$\theta_{c.m.}$ (deg)

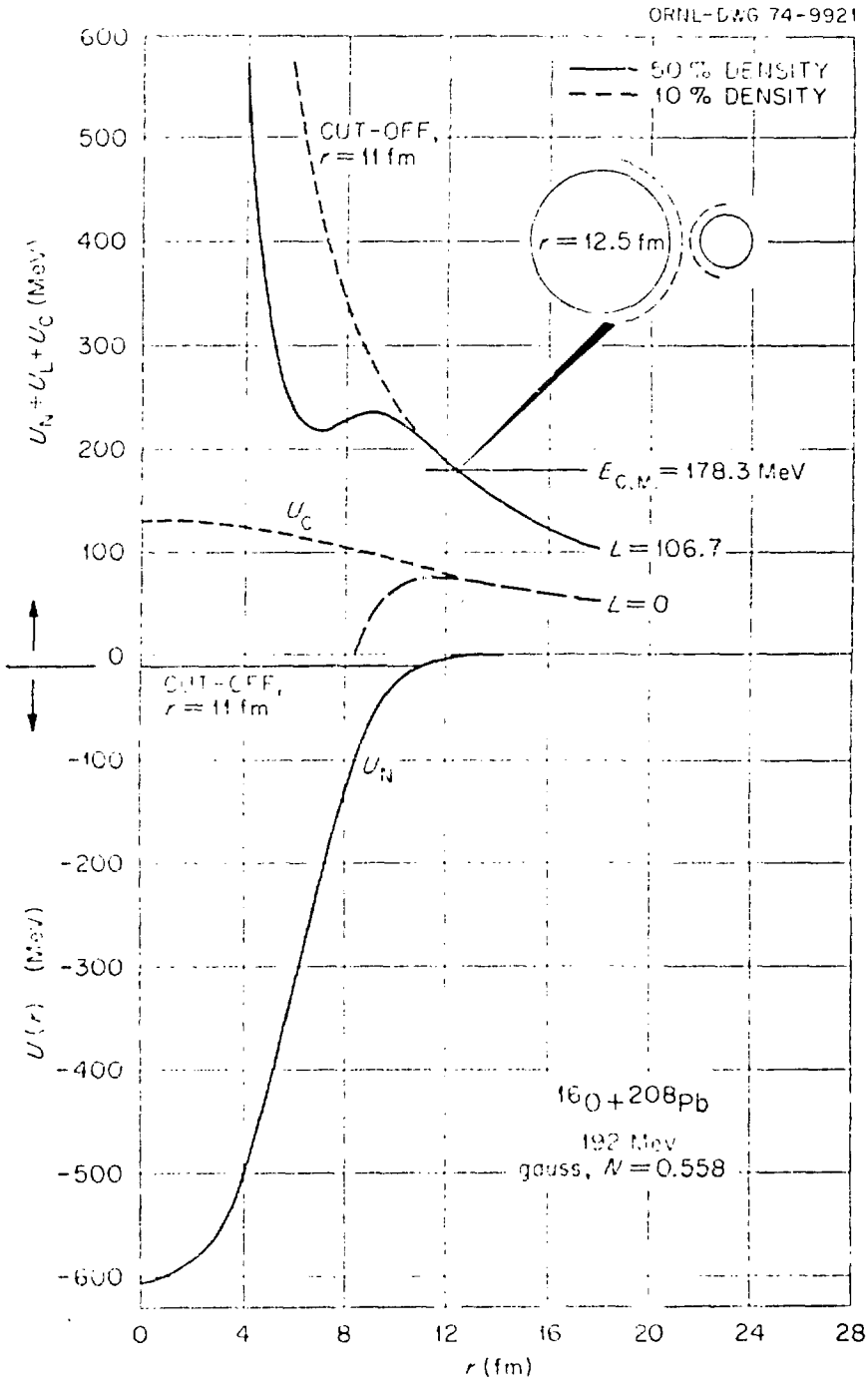
ORNL-DWG 74-9921
50 % DENSITY
10 % DENSITY
CUT-OFF, r = 11 fm
r = 12.5 fm
E C.M. = 178.3 MeV
L = 106.7
L = 0
U C
U N
CUT-OFF, r = 11 fm
16O + 208Pb
192 Mev
gauss, N = 0.558
U N + U L + U C (Mev)
U(r) (Mev)
r (fm)
600
500
400
300
200
100
0
-100
-200
-300
-400
-500
-600
0
4
8
12
16
20
24
28

6

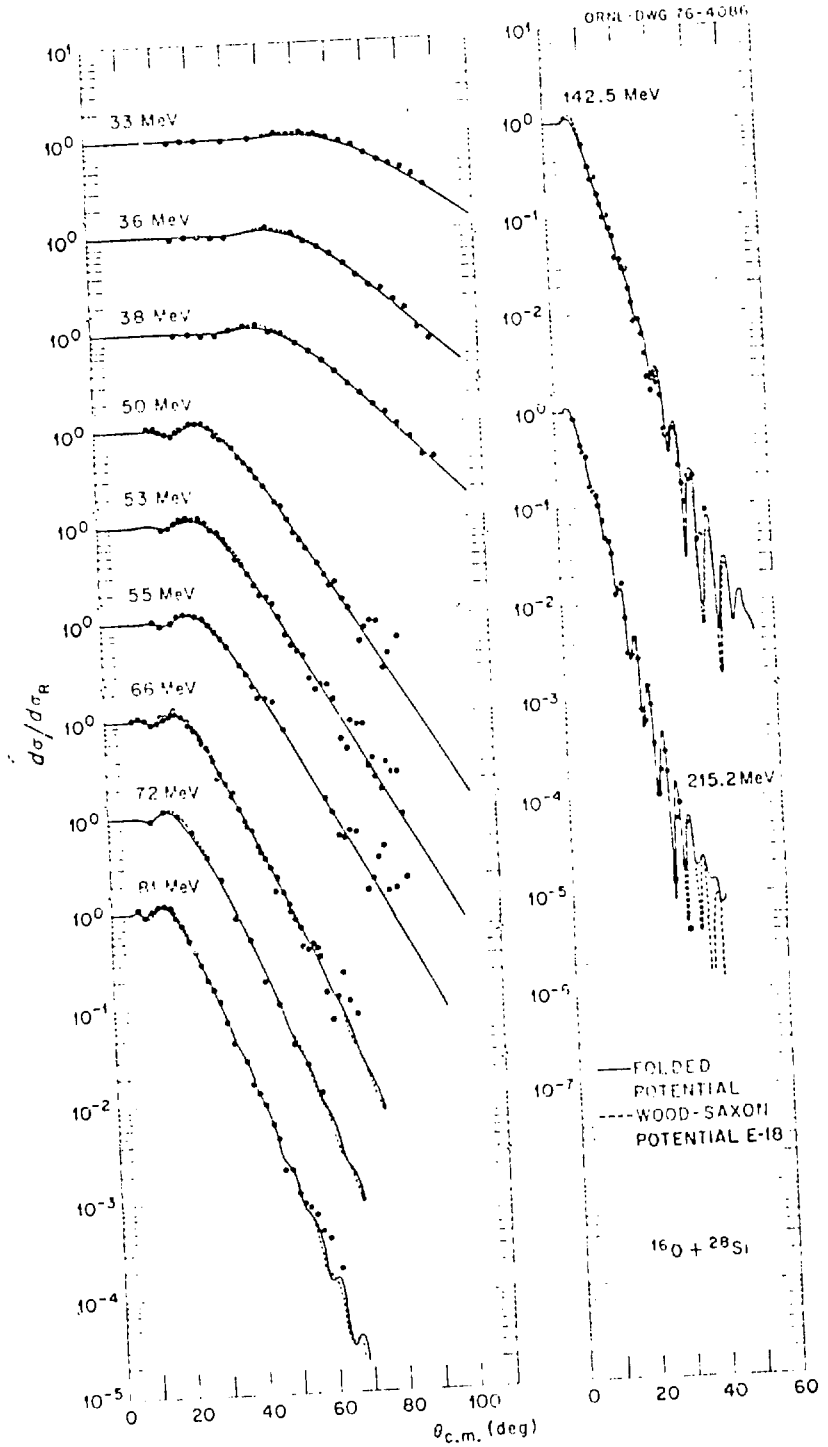
ORNL-DWG 76-4086
33 MeV
36 MeV
38 MeV
50 MeV
53 MeV
55 MeV
66 MeV
72 MeV
81 MeV
142.5 MeV
215.2 MeV
$d\sigma/d\sigma_R$
$\theta_{c.m.}$ (deg)
—FOLDED POTENTIAL
----WOOD-SAXON POTENTIAL E-18
$^{16}O + ^{28}Si$

7

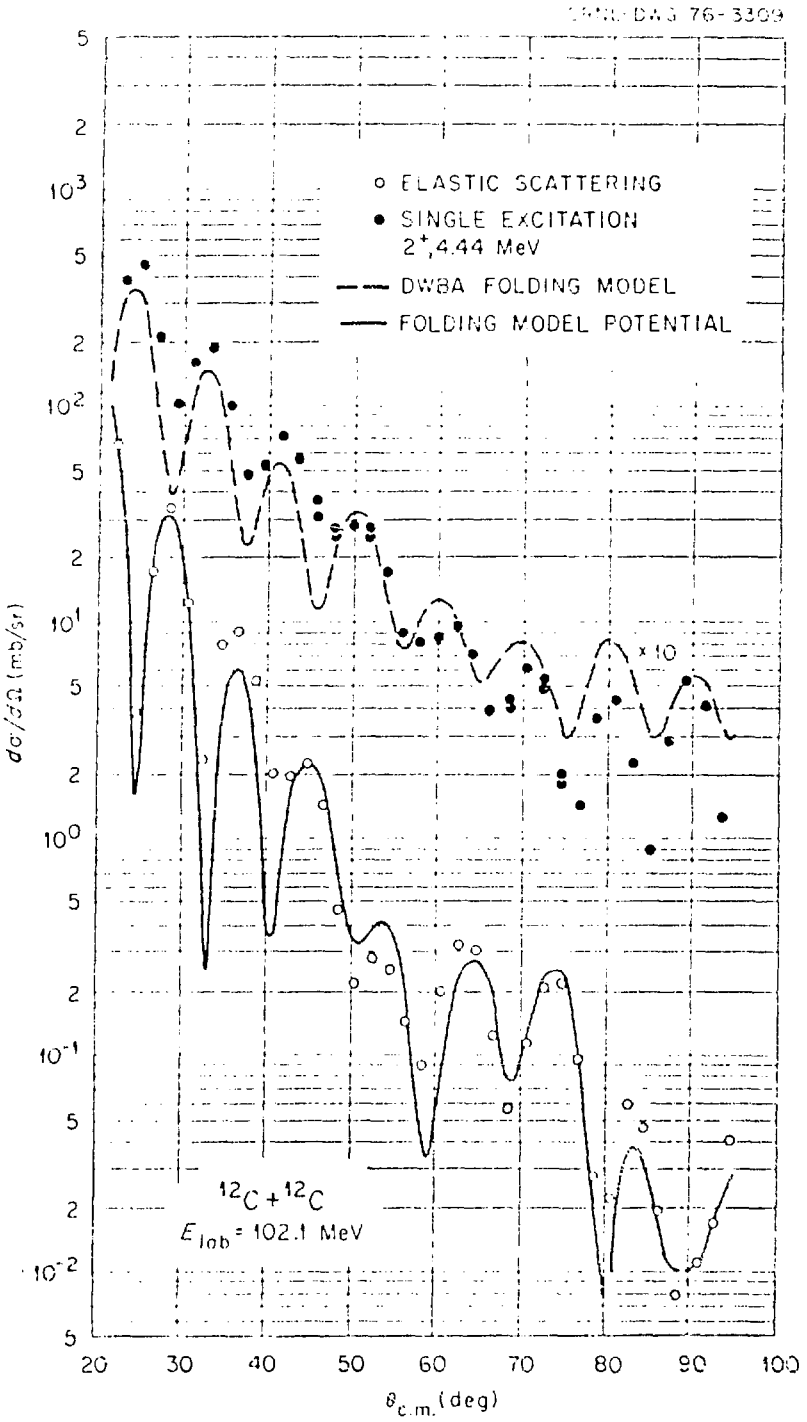
ORNL-DWG 76-3309
ELASTIC SCATTERING
SINGLE EXCITATION
2+,4.44 MeV
DWBA FOLDING MODEL
FOLDING MODEL POTENTIAL
x10
12C + 12C
Elab = 102.1 MeV
dσ/dΩ (mb/sr)
θc.m. (deg)

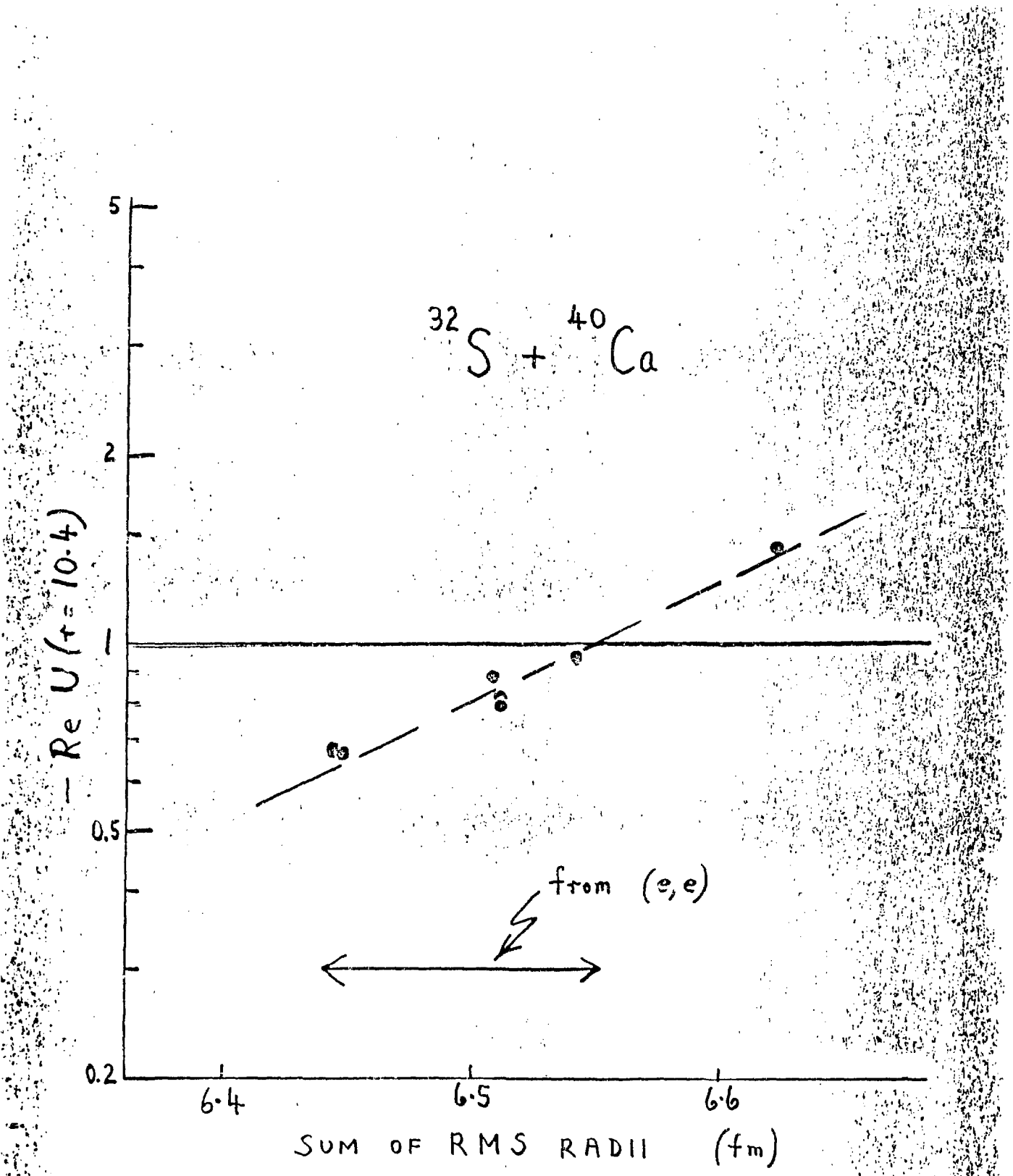
$^{32}S + ^{40}Ca$
5
2
1
0.5
0.2
$-\mathrm{Re}\,U(r = 10.4)$
from (e,e)
6.4
6.5
6.6
SUM OF RMS RADII (fm)

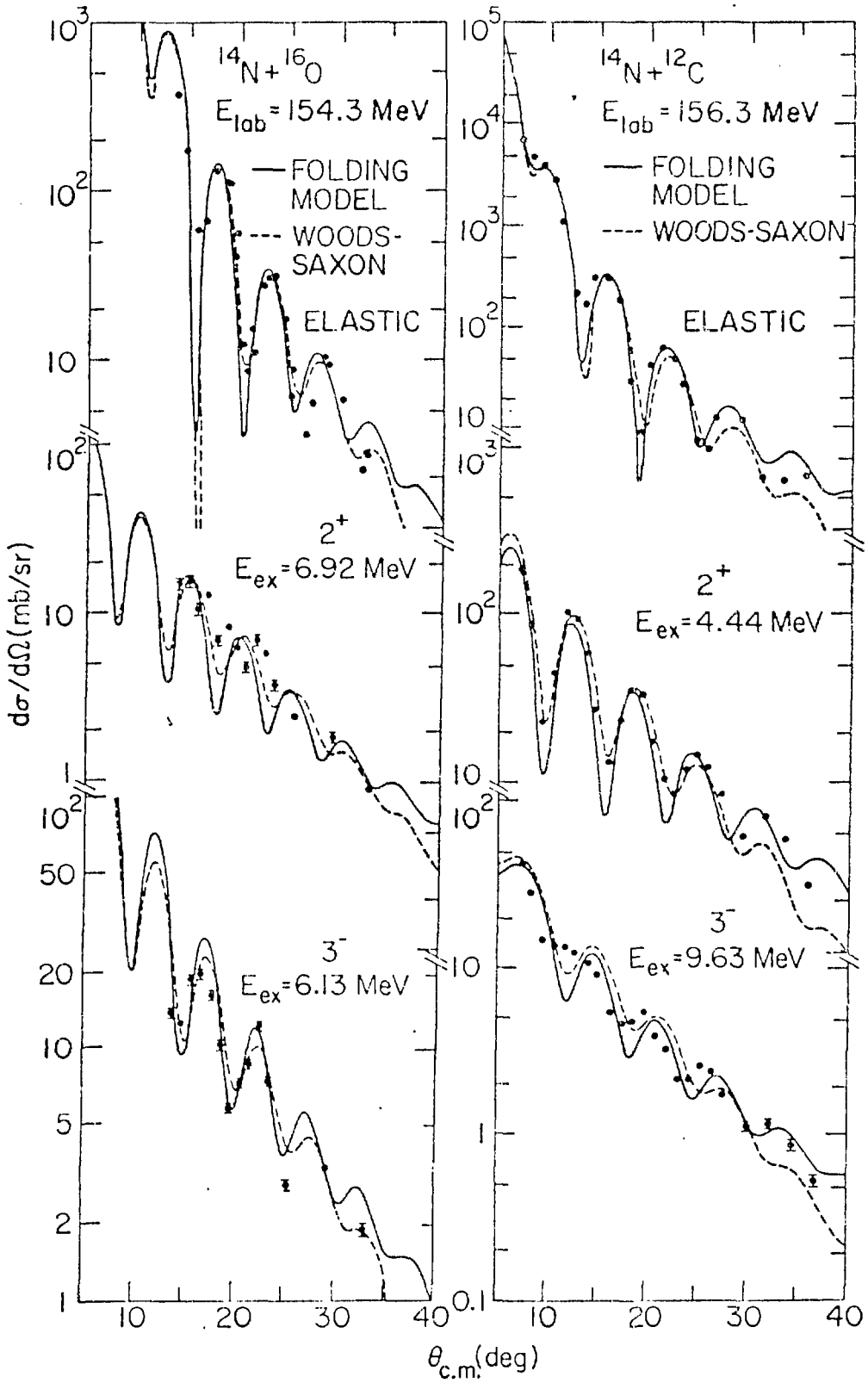
$^{14}N + ^{16}O$
E_{lab} = 154.3 MeV
— FOLDING MODEL
--- WOODS-SAXON
ELASTIC
2^+
E_{ex} = 6.92 MeV
3^-
E_{ex} = 6.13 MeV
$^{14}N + ^{12}C$
E_{lab} = 156.3 MeV
— FOLDING MODEL
---- WOODS-SAXON
ELASTIC
2^+
E_{ex} = 4.44 MeV
3^-
E_{ex} = 9.63 MeV
$d\sigma/d\Omega$ (mb/sr)
$\theta_{c.m.}$ (deg)

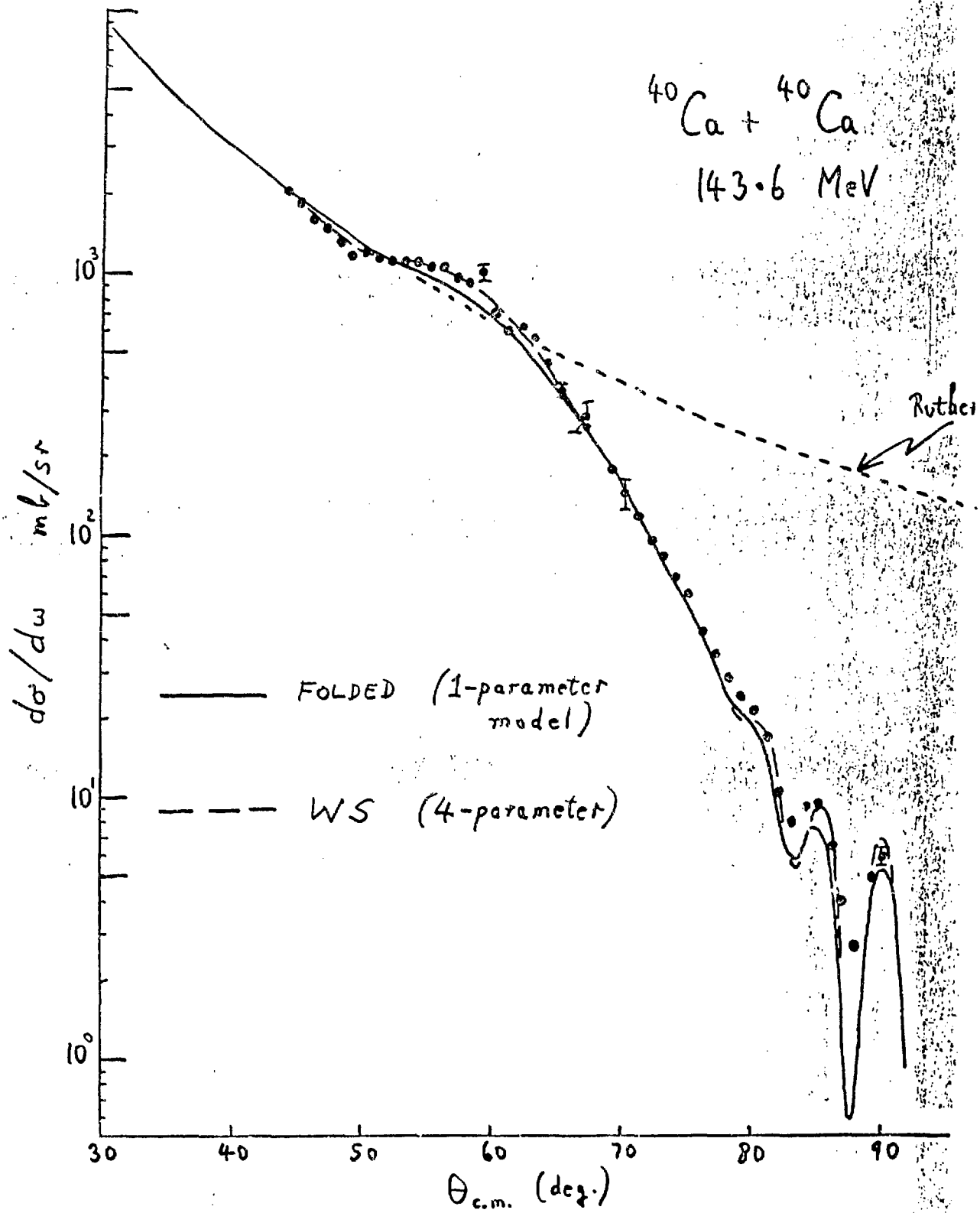
$^{40}Ca + ^{40}Ca$
143.6 MeV
Ruther
FOLDED (1-parameter model)
WS (4-parameter)
$d\sigma/d\Omega$ mb/sr
10^3
10^2
10^1
10^0
30
40
50
60
70
80
90
$\theta_{c.m.}$ (deg.)

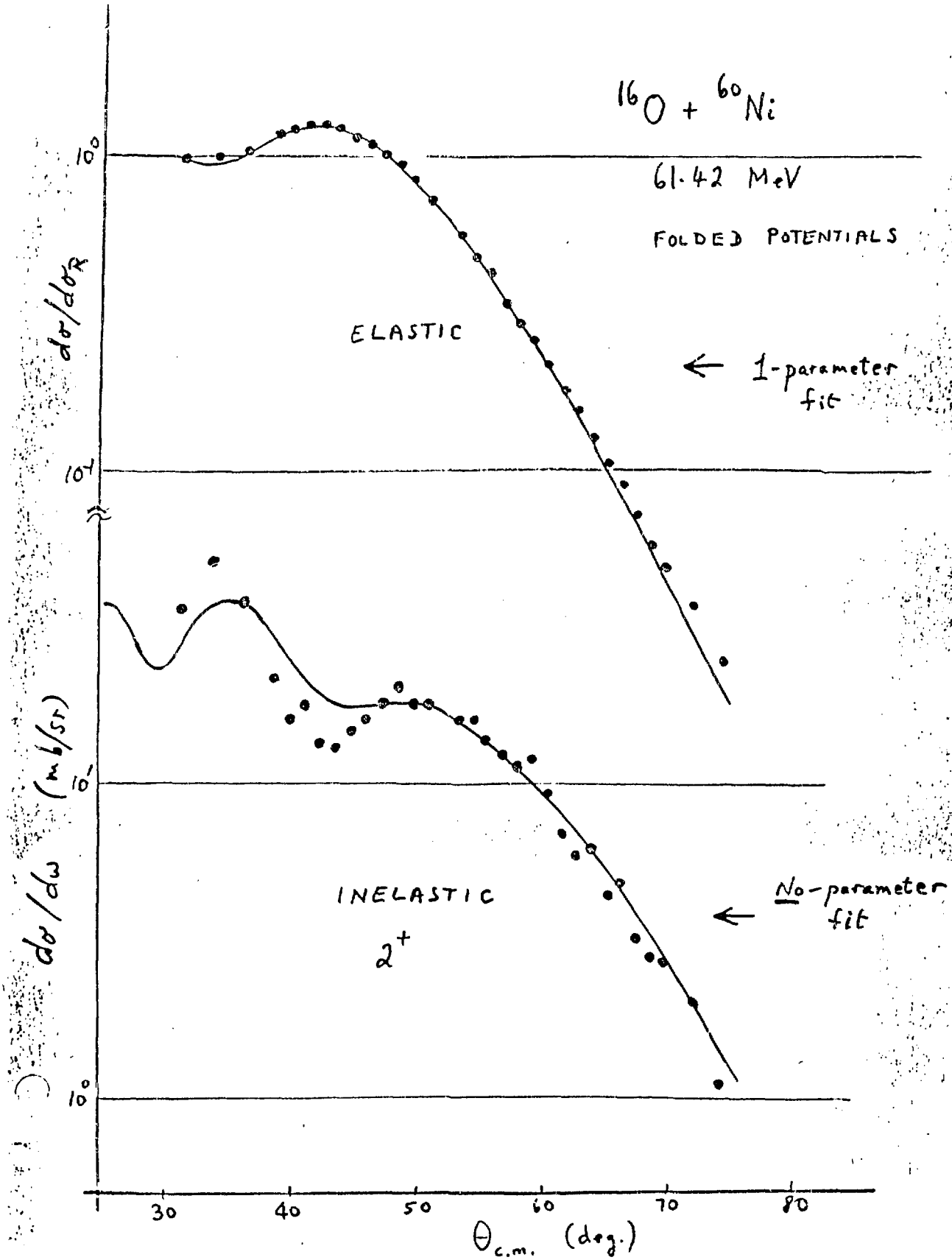
$^{16}O + ^{60}Ni$
61.42 MeV
FOLDED POTENTIALS
ELASTIC
← 1-parameter fit
INELASTIC
2^+
← No-parameter fit
$d\sigma/d\sigma_R$
$d\sigma/d\Omega$ (mb/sr)
10^0
10^{-1}
10^1
10^0
30
40
50
60
70
80
$\theta_{c.m.}$ (deg.)

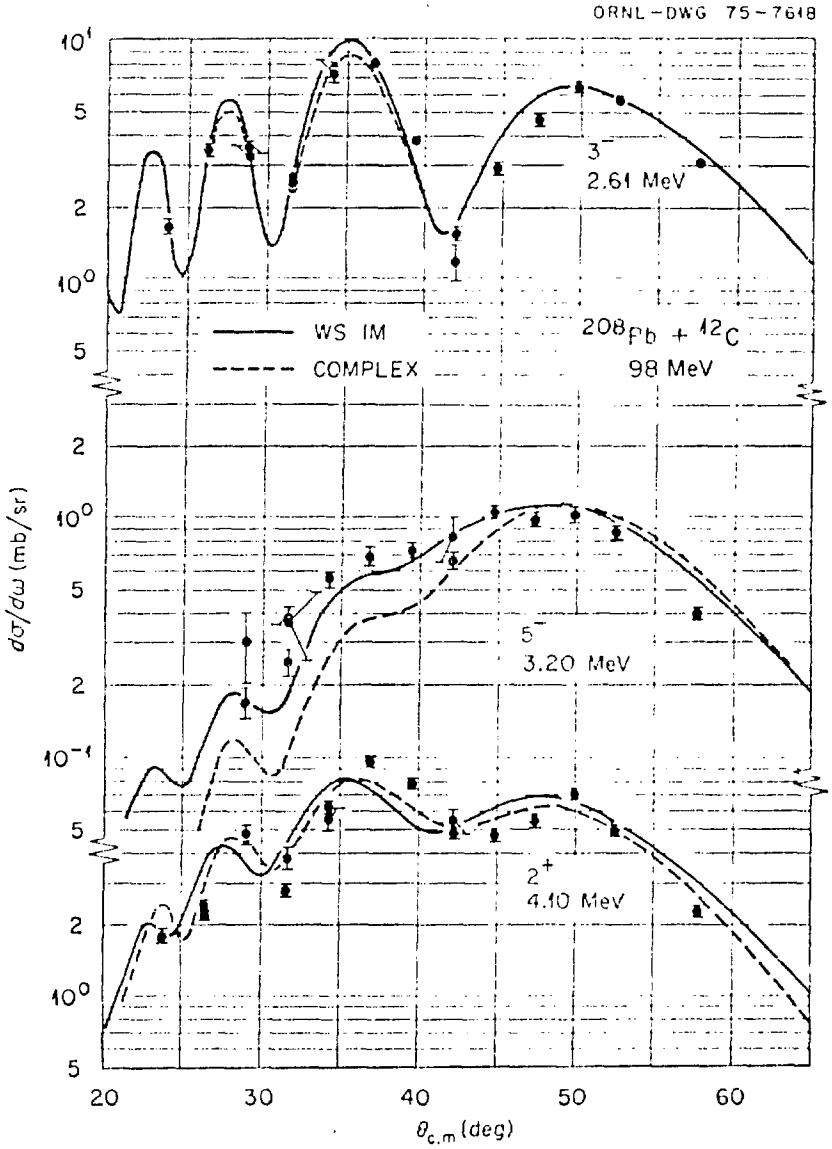
ORNL-DWG 75-7618
10^1
5
2
10^0
5
2
10^0
5
2
10^{-1}
5
2
10^0
5
$d\sigma/d\omega$ (mb/sr)
WS IM
COMPLEX
$^{208}Pb + ^{12}C$
98 MeV
3^-
2.61 MeV
5^-
3.20 MeV
2^+
4.10 MeV
20
30
40
50
60
$\theta_{c.m}$ (deg)

13